Membrane-inserted conformation of transmembrane domain 4 of divalent-metal transporter

Hongyan LI*, Fei LI†, Hongzhe SUN†[1,2] and Zhong Ming QIAN*[2]

*Department of Applied Biology and Chemical Technology, The Hong Kong Polytechnic University, Kowloon, Hung Hom, Hong Kong, Peoples' Republic of China, and †Department of Chemistry and Open Laboratory of Chemical Biology, The University of Hong Kong, Pokfulam Road, Hong Kong, Peoples' Republic of China

Divalent-metal transporter 1 (DMT1) is involved in the intestinal iron absorption and in iron transport in the transferrin cycle. It transports metal ions at low pH (≈5.5), but not at high pH (7.4), and the transport is a proton-coupled process. Previously it has been shown that transmembrane domain 4 (TM4) is crucial for the function of this protein. Here we provide the first direct experimental evidence for secondary-structural features and membrane insertions of a 24-residue peptide, corresponding to TM4 of DMT1 (DMTI-TM4), in various membrane-mimicking environments by the combined use of CD and NMR spectroscopies. The peptide mainly adopts an α-helical structure in trifluoroethanol, SDS and dodecylphosphocholine micelles, and dimyristoyl phosphatidylcholine and dimyristoyl phosphatidylglycerol small unilamellar vesicles. It has been demonstrated from both Hα secondary shifts and nuclear-Overhauser-enhancement (NOE) connectivities that the peptide is well folded into an α-helix from Val^{8} to Lys^{23} in SDS micelles at pH 4.0, whereas the N-terminus is highly flexible. The α-helical content estimated from NMR data is in agreement with that extracted from CD simulations. The highest helicity was observed in the anionic phospholipids {1,2-dimyristoyl-*sn*-glycero-3-[phospho-*rac*-(1-glycerol)]}, indicating that electrostatic attraction is important for peptide binding and insertion into the membranes. The secondary-structural transition of the peptide occurred at pH 4.3 in the 2,2,2-trifluoroethanol (TFE) water mixed solvent, whereas at a higher pH value (5.6) in SDS micelles, DMT1-TM4 exhibited a more stable structure in SDS micelles than that in TFE in terms of changing the pH and temperature. PAGE did not show high-molecular-mass aggregates in SDS micelles. The position of the peptide relative to SDS micelles was probed by the effects of 5- and 16-doxylstearic acids on the intensities of the peptide proton resonances. The results showed that the majority of the peptide is inserted into the hydrophobic interior of SDS micelles, whereas the C-terminal residues are surface-exposed. The ability of DMT1-TM4 to assume transmembrane features may be crucial for its biological function *in vivo*.

Key words: divalent-metal transporter 1 (DMT1), circular dichroism (CD), detergent, NMR, phospholipid vesicles, secondary structure.

INTRODUCTION

Iron is essential for almost all living organisms and plays a part in a wide range of metabolic processes. However, it can also be harmful when it reacts with oxygen to generate toxic radicals. Proteins usually sequester iron to reduce this threat. In blood plasma, iron is thought to be transported into cells by transferrin via receptor-mediated endocytosis [1,2], a process that has also been suggested for transport of several other metal ions and drugs [3,4]. Failure to maintain appropriate levels of iron in humans is a feature of hereditary haemochromatosis, iron-deficiency anaemia, and certain neurodegenerative diseases [5,6].

Recently, several new genes related to iron homoeostasis have been identified, including divalent-metal transporter 1 (DMT1) [7–9]. DMT1 encodes the transporter responsible for importing iron from the gut into the enterocytes and also across the endosomal membrane in the transferrin cycle [7,7a,10]. Integral DMT1 consists of 561 amino acids and has unusually broad substrate specificity, ranging from essential divalent metals such as Fe^{2+}, Zn^{2+}, Mn^{2+}, Cu^{2+} and Ni^{2+} to toxic metals such as Pb^{2+} and Cd^{2+}. Transport of these metal ions occurs at pH 5.5, but not at 7.4, and is a proton-coupled process [7,7a]. DMT1 is a member of the natural-resistance-associated macrophage protein family (Nramp2) and is highly hydrophobic, with 12 putative transmembrane domains. The biological importance of this transporter has been shown by its involvement in two naturally occurring animal mutants of iron metabolism. It has been shown previously that missense mutations occurring within transmembrane domain 4 (TM4) of DMT1 are causative mutations in microcytic-anaemic mice and Belgrade rats, which have severe defects in intestinal iron absorption and erythroid iron utilization [7,7a,10,11]. This suggests that TM4 of DMT1 (designated as DMT1-TM4) may have a unique and important biological function. The sequence of this domain is characterized by a high degree of hydrophobicity and is highly conserved among different species (Figure 1).

Despite the functional importance of DMT1-TM4, no studies have been undertaken thus far to assess the structure of either this segment or the entire DMT1 molecule. Generally, it is difficult to obtain atomic-resolution structures for integral membrane proteins, owing to their intractability to crystallization and the slow reorientation of proteins within the membrane region, impeding NMR structural analysis. However, the approaches that provide easily accessible, qualitative structural information

Abbreviations used: CMC, critical micelle concentration; DMPC, dimyristoyl phosphatidylcholine (1,2-dimyristoyl-*sn*-glycero-3-phosphocholine); DMPG, dimyristoyl phosphatidylglycerol {1,2-dimyristoyl-*sn*-glycero-3-[phospho-*rac*-(1-glycerol)]}; DMT1, divalent (=bivalent)-metal transporter; DMT1-TM4, transmembrane domain 4 of DMT1; DPC, dodecylphosphocholine; HFIP, 1,1,1,3,3,3-hexafluoropropan-2-ol; MRE, mean residue ellipticity; NOE, nuclear Overhauser enhancement; Nramp, natural-resistance-associated macrophage protein; RMSD, root-mean-square deviation (between experimental results and calculations); SUVs, small unilamellar vesicles; TFA, trifluoroacetic acid; TFE, 2,2,2-trifluoroethanol.

[1] To whom correspondence should be addressed (e-mail bczmqian@polyu.edu.hk).

[2] The groups of Dr Sun and Dr Qian contributed equally to the work.

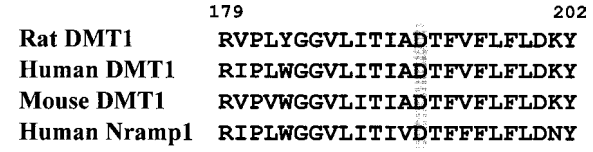

Figure 1 Sequence alignment of the putative DMT1-TM4 from three different species with that of human Nramp1

GeneBank® accession numbers are AF008439 (rat DMT1), L37347 (human DMT1), NM_008732 (mouse DMT1) and L32185 (human Nramp1). A conserved aspartic acid residue is highlighted.

can be extremely useful for identifying common folds and in guiding complete structure determination [12,13]. Indeed, three-dimensional structural models of lactose permease, a 12-transmembrane helix bundle that transduces free energy, have been derived recently on the basis of its transmembrane topology, secondary structure and numerous interhelical contacts without using crystals [14]. Model transmembrane peptides have been widely used to investigate structure and function in several integral membrane proteins [12,15–20]. It has been shown previously that transmembrane sequences can assume membrane-integrated conformations and even form native-like inter-peptide interactions, yielding functional model structures [20,21]. In the present study, we have used both CD and NMR spectroscopies to explore secondary-structural features of a synthetic peptide that mimics the sequence of rat DMT1-TM4 in different membrane-mimetic environments, including 2,2,2-trifluoroethanol (TFE), TFE/water mixtures, SDS and dodecylphosphocholine (DPC) micelles, as well as dimyristoyl phosphatidylcholine (DMPC), and dimyristoyl phosphatidylglycerol (DMPG) vesicles. The effects of pH, temperature and concentration on the secondary structure have also been investigated in detail. The topology of the peptide relative to SDS micelles was investigated by the effects of stearic acid-derived spin labels on the intensities of NMR signals. The potential oligomeric state of the peptide in SDS micelles was also investigated using PAGE. Our results indicate that the DMT1-TM4 peptide adopts a predominantly α-helical structure in all membrane-mimicking environments studied and is likely to be inserted into the micelles with the C-terminus exposed.

MATERIALS AND METHODS

Materials

The DMT1-TM4 peptide (RVPLYGGVLITIADTFVFLFLDKY-OH), corresponding to residues 179–202 of DMT1, was synthesized using solid-phase methodology and was purified by HPLC on a Zorbax SB Phenyl reverse-phase column (Bio-Peptide Co., LLC, San Diego, CA, U.S.A), using 0.1 % 2,2,2-trifluoroacetic acid (TFA)/water and 0.1 % TFA/acetonitrile as solvents. The purity of the peptide was assessed by both MS and analytical HPLC to be > 95 %. Serva Blue G was obtained from Serva. Low-molecular-mass markers were obtained from Amersham Biosciences.

TFE, 1,1,1,3,3,3-hexafluoropropan-2-ol (HFIP), TFA, Tricine, SDS, DPC, DMPG, DMPC, 5-doxylstearic acid and 16-doxylstearic acid were obtained from Sigma, in the highest available purity, and were used directly without further treatment.

Sample preparation

The peptide was first dissolved in TFA (≈100 mg/ml) and then dried under a stream of nitrogen. The stock solution of the peptide (≈2 mg/ml) was then prepared in TFE. This resulted in the solubilization of almost 80 % of the peptide, with the remainder removed by low-speed centrifugation. The concentration of the stock solution was determined from amino acid analysis. For the various TFE titration experiments, the stock solution of the peptide was diluted using different volumes of water and TFE to give rise to different percentages of TFE.

The peptide was incorporated into SDS and DPC micelles using a procedure described previously [22]. Briefly, for CD experiments, the peptide, which was dissolved in TFE, was added to an equal volume of an aqueous solution containing various amounts of SDS or DPC, and water was added to yield a 16 : 1 ratio (water/TFE, v/v). The samples were mixed by vortex-mixing for 2 s and then freeze-dried. The resulting dry powder was rehydrated with either water or buffer solutions and the pH was adjusted by the addition of a very small amount of HCl or NaOH. The NMR samples were prepared by mixing 3 mg of DMT1-TM4 peptide, dissolved in 0.2 ml of HFIP, with 0.2 ml of concentrated [^{2}H]SDS solution. Similarly, the mixture was further diluted with water to produce a water/TFE ratio of 16 : 1 and was subjected to freeze-drying. The resulting powder was then dissolved in 0.6 ml of water containing 10 % ^2H_2O. The final SDS concentration was 300 mM. The pH was adjusted to 4–6 by the addition of a small amount of NaOH or HCl.

Incorporation of the peptide into DMPC and DMPG vesicles was carried out as previously reported [23,24]. A solution of the peptide in TFE was mixed with DMPC or DMPG in chloroform/methanol (2 : 1, v/v) to give a lipid/peptide molar ratio of 200 : 1. The organic solvent was evaporated under nitrogen until a lipid film was obtained. The film was then further dried under vacuum or freeze-dried overnight. It was then hydrated with MilliQ water and vortex-mixed for ≈30 min, with caution taken to ensure that the temperature was maintained at 10 °C above the phase-transition temperature of the lipids. The vesicle suspension was then sonicated using a bath-type sonicator until the initially cloudy solution became clear. During the period of sonication, the temperature of the water bath was carefully maintained at around 30 °C to prevent potential damage to the lipid vesicles. The resulting small unilamellar vesicles (SUVs) were used directly for spectroscopy measurements. Freshly prepared lipid was used so that oxidation would be minimized.

CD spectroscopy

Far-UV CD spectra (190–260 nm) of the peptide were recorded on either Jasco J-810 or J-720 spectropolarimeters. These instruments had been calibrated previously for wavelength using benzene vapour, and for optical rotation using *d*-10-camphorsulphonic acid. A cell with a path length of 1 mm was used. A thermostatically controlled cell holder and a Thermo NESLAB (Portsmouth, NH, U.S.A.) RTE-111M temperature controller were used to maintain the desired temperatures. For experiments at different temperatures, measurements were made between 5 and 70 °C, in 5 °C increments, with 20 min equilibration at each temperature. The parameters used were as follows: bandwidth, 1 nm; step resolution, 0.1 nm; scan speed, 50 nm/min; response time, 0.25 s. Each spectrum was obtained after an average of four to six scans. The peptide concentration was typically 10–20 μM in TFE, in various ratios of lipid micelle solutions, or in lipid vesicles. Prior to calculation of the final ellipticity, all spectra were corrected by subtraction

of spectra obtained for peptide-free samples (containing only solvent, detergents or vesicles). Spectra were then smoothed using adjacent averaging or a FFT (fast Fourier transform) filter. CD intensity is expressed as mean residue ellipticities (θ_{MRE}, in degrees $\cdot$ cm^2 $\cdot$ dmol^{-1}) according to the following equation:

$$\theta_{MRE} = \theta_{mdeg}/10icn$$

where θ_{mdeg} is the measured ellipiticity in millidegrees, i is the cell path length in cm, c is the molar concentration of the protein or peptide, and n is the number of amino acid residues in the peptide.

NMR spectroscopy

The ^{1}H NMR spectra were recorded on a Bruker AV600 spectrometer operating at 600.13 MHz. Homonuclear TOCSY [25] and NOESY [26] spectra were acquired at 25 °C with water suppression achieved using the WATERGATE technique [27]. Spectra were collected with 512 data points in F1, 2K data points in F2, and 32–80 transients. TOCSY spectra were acquired using the MLEV-17 pulse sequence [25] at spin-lock times of 50 and 75 ms. A series of NOESY spectra was recorded with a mixing time of 100, 200 and 250 ms respectively. All two-dimensional spectra were recorded in a phase-sensitive absorption mode using States-TPPI in F1. The spectra were processed using XWINNMR software, and prior to Fourier transformation the data were zero-filled to 2K data points in each dimension.

To determine the insertion of DMT1-TM4 into micelles, the effect of 5- and 16-doxylstearic acids on ^{1}H resonances was investigated. After recording of the TOCSY spectrum with a spin-lock time of 50 ms in the absence of the spin labels, the NMR samples were mixed with 20 μl of freshly prepared spin labels solubilized in [$^2H_4$]methanol to yield concentrations of 5 mM, corresponding to approximately one spin-label per micelle. TOCSY spectra were then recorded.

pH measurements

The pH values for solutions of DMT1-TM4 peptide in different percentages of TFE/water, or in the presence of detergent or phospholipids, were measured using a Corning 440 pH-meter, equipped with an Aldrich micro-combination electrode, calibrated with standard buffers (pH 4.00 and 7.00).

Analyses of secondary structure

Quantitative estimations of the secondary-structure contents were made using the CDPro software package, which includes the programs CDSSTR, CONTIN and SELCON3 (http://lamar.colostate.edu/~sreeram/CDPro) [28]. The version of CONTIN used had been modified to include the variable selection of reference proteins in a locally linearized model (CONTINLL) [29]. We used these three programs to analyse our CD spectra, and found that CONTINLL gave rise to a best fit with the lowest root-mean-square deviation (RMSD) between experimentally derived and calculated points; while SELCON3 and CDSSTR gave negative fractions in some calculations. Results with a 43-protein set are reported in the Tables, and other reference protein sets, such as 29, 37, 42 and 48, were also tested and gave rise to comparable results. The α-helical fractions extracted from the CDPro program are in a relatively good agreement with those calculated based on empirical methods using ellipticities at either 208 or 222 nm [30,31].

Tricine/SDS/PAGE

The potential oligomeric state of DMT1-TM4 in both 17 and 100 mM SDS was investigated by gel electrophoresis. A Tricine buffer system [32] was employed, but increasing the SDS concentration to 0.5 % (17 mM) in the gel, which is above the critical micelle concentration. The peptide was solubilized in 10 mM Tris buffer at pH 7.4 in the presence of 17 or 100 mM SDS as described above ('Sample preparation'). The samples were diluted with 4 × SDS loading buffer containing the tracking dye Serva Blue G, and were either loaded directly or boiled for 5 min before loading on to a 16.5 %-polyacryalamide/Tricine/SDS gel. They were then separated at a constant 120 V at room temperature. After gel electrophoresis, the gel was placed in a solution containing 50 % methanol and 40 % acetic acid for 30 min prior to staining. The peptide was visualized by staining with Coomassie Brilliant Blue.

RESULTS

Secondary-structural studies of DMT1-TM4 in membrane-mimetic environments

The DMT1-TM4 peptide is insoluble in water and many common organic solvents, such as methanol, ethanol and chloroform, owing to the highly hydrophobic nature of the peptide. Therefore choosing suitable solvents is essential not only for solubilizing the peptide, but also for mimicking biological membranes.

In TFE and TFE/water mixed solvents

The CD spectra of the DMT1-TM4 peptide measured in TFE/water mixtures ranging from 80 % TFE/20 % water to 10 % TFE/90 % water at pH 5.5 are shown in Figure 2. At low percentages of TFE, the spectra are characterized by a broad negative band at around 220 nm and a positive band at around 190 nm, attributable to the presence of a mixture of α-helix and β-structures. At increasing concentrations of TFE, a helical structure was induced, as indicated by the appearance of double minima at 208 and 222 nm and a positive maximum at 195 nm (Figure 2). The α-helical content increased with increasing TFE

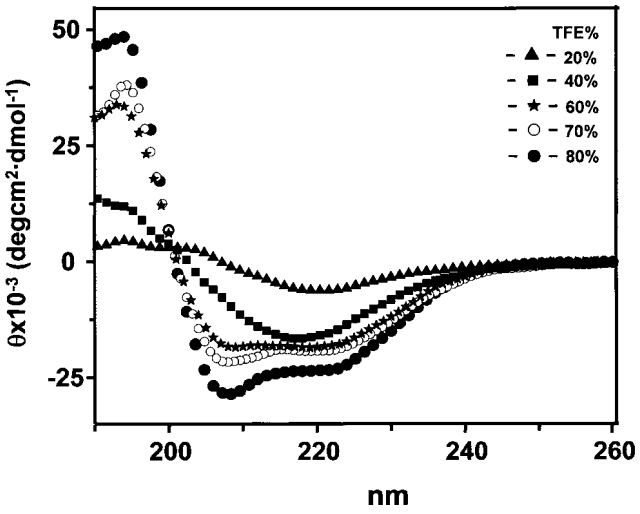

Figure 2 CD spectra of DMT1-TM4 in TFE/water mixed solvents

Samples were diluted from the stock solution of the peptide in TFE with water or TFE. The fraction of α-helix increases with the increase in TFE percentages. Abbreviation: degcm^2, degrees $\cdot$ cm^2.

Table 1 Secondary-structural analyses of the DMT1-TM4 peptide in TFE/water mixed solvents

The results were obtained from CONTINLL with a 43-reference set using CDPro software.

	Secondary structure (%)†				
TFE (%)*	Helix	Strand	Turn	Unordered	RMSD
10	3	43	22	32	0.075
20	7	37	23	33	0.067
30	17	27	28	28	0.076
40	18	29	25	28	0.195
50	32	14	27	27	0.209
60	51	8	19	22	0.082
70	62	3	16	19	0.278
80	74	2	8	16	0.228
100	67	2	10	21	0.238

* The pH was adjusted to 5.5, except in the presence of 100 % TFE.

† For convenience of data interpretation, we added the distorted and regular components of both helical and strand secondary-structural elements together to obtain overall helical and strand structures in both Tables 1 and 2.

concentrations, as shown in Table 1. The α-helical contents increased significantly from 3 % at 10 % TFE, to 74 % at 80 % TFE. In contrast with the striking rise in α-helical fractions, there was a general decrease in the β-structures, from 65 % at 10 % TFE to 10 % at 80 % TFE. Similarly, the unordered structure also decreased with increasing TFE concentrations (Table 1).

In SDS and DPC detergents

SDS is a surfactant that can provide a hydrophobic environment for polypeptides and proteins. The effects of negatively charged SDS on the secondary structure of DMT1-TM4 were investigated at pH 5.5, at ambient temperature, with SDS concentrations ranging from 2 to 200 mM. It can be seen from Figure 3(A) that at low concentrations of SDS (2 and 4 mM), the spectra were characterized by one negative maximum at 216 nm and one positive maximum at $\approx$190 nm, indicative of a mixture of α-helix and β-structures, whereas at high SDS concentrations (8, 20, 50, 100 and 200 mM), the CD spectra showed characteristics of a predominantly α-helical conformation. The α-helical content increased with increasing SDS concentrations and remained constant at SDS concentrations above 8.0 mM. It has been previously noted that submicellar concentrations of SDS tend to induce a β-strand conformation, whereas an α-helical structure is more likely to be induced at or above micellar concentrations (8.1 mM) [33,34]. Quantitative analysis of the fraction of secondary structures showed substantial 59 and 50 % β-structure induced by 2 and 4 mM SDS respectively. The percentage of β-structures in micellar concentrations of SDS decreased dramatically to 9 %. Conversely, the fraction of α-helical content was found to increase considerably to 72 % in micellar concentrations of SDS, compared with 14 and 24 % at submicellar concentrations of 2 and 4 mM respectively (Table 2).

To examine the possible influence of detergent charge on the peptide structure, samples of DMT1-TM4 in the zwitterionic detergent DPC were investigated (Figure 3B). Similar to those obtained in the SDS system, the spectra of DMT1-TM4 in 0.5 and 1 mM DPC, which is below the critical micelle concentration (CMC) of DPC (1.1 mM) [35], showed characteristics of β-structures. However, at micellar DPC concentrations, spectral features typical for α-helical structures became apparent. Quantitative analysis using CDPro software (Table 2) verified that DMT1-TM4 adopts mainly β-structures at submicellar DPC

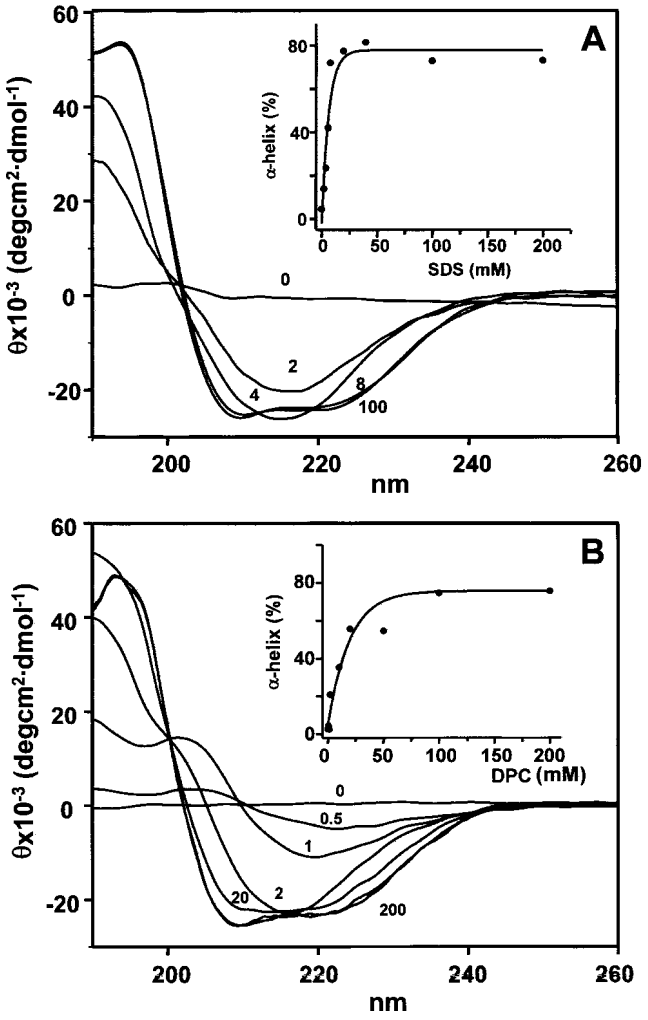

Figure 3 Effects of SDS and DPC on the secondary structure of DMT1-TM4

(**A**) CD spectra of DMT1-TM4 in aq. SDS solution at pH 5.5 with increasing concentrations of SDS from 2 to 200 mM. The inset shows helicity as a function of SDS concentration. (**B**) CD spectra of 12 μM peptide in aq. DPC solution at pH 5.5 with increasing concentrations of DPC from 0.5 to 200 mM. The inset shows helicity as a function of DPC concentration. Abbreviation: degcm^2, degrees · cm^2.

concentrations (64 and 58 % at 0.5 and 1 mM concentrations of DPC respectively). Significant amounts of unordered structures were also observed under these conditions. Conversely, the α-helical content increased significantly with increasing DPC concentrations, 75 % in 100 mM DPC, compared with less than 4 % at submicellar concentrations (Table 2). In contrast with the peptide in SDS solution, the helicity of DMT1-TM4 increased slowly with increasing DPC concentrations, even above the CMC, and remained unchanged at DPC concentrations over 100 mM (Table 2).

In DMPC and DMPG phospholipids

Membrane mimetics such as TFE or SDS have the intrinsic property of inducing peptides to adopt α-helical conformations. To avoid an overestimation of such effects, we studied the secondary structure of DMT1-TM4 in the presence of lipid membranes. In order to investigate the nature of the peptide–lipid interactions, particularly with the lipid head groups, anionic (DMPG) and zwitterionic (DMPC) phospholipids were used in

Table 2 Summary of structural analyses of the DMT1-TM4 peptide in various membrane-mimicking environments using CONTINLL with a 43-reference protein set*

Environment	Concn. (mM)	pH	Secondary structure (%)				RMSD
			Helix	Strand	Turn	Unordered	
SDS	2	5.5	14	33	26	27	0.157
	4	5.5	24	32	18	26	0.134
	8.1	5.5	72	2	7	19	0.115
	20	5.5	77	0	6	17	0.151
	40	5.5	80	0	4	16	0.162
	100	5.5	73	1	7	19	0.178
	200	5.5	73	1	7	19	0.219
DPC	0.5	5.5	4	41	23	32	0.073
	1.0	5.5	3	28	30	39	0.342
	2.0	5.5	21	37	14	28	0.207
	10	5.5	35	12	20	33	0.344
	20	5.5	56	6	0	38	0.178
	100	5.5	75	1	8	16	0.171
	200	5.5	76	1	8	15	0.163
DMPC	3.8	5.0	47	23	12	18	0.273
		7.4	16	44	24	16	0.337
DMPG	3.8	5.0	82	2	4	12	0.286
		7.4	65	11	9	15	0.190

* Peptide concentrations were typically in the range of 10–20 μM.

the present study. In order to eliminate the differential light-scattering and absorption-flattening artifacts in CD measurement, which was noticed in other membrane samples [36], SUVs with a high lipid-to-protein ratio (200 : 1) were used for the study. DMT1-TM4 (19 μM) was reconstituted in $\approx$3.8 mM DMPC or DMPG to SUVs, and the far-UV CD spectra are shown in Figure 4. It can be seen that the peptide adopted predominantly an α-helical conformation in DMPG, with characteristic double minima at 208 and 222 nm, while in DMPC the spectra obtained were more complex, with broader and deeper minima that extended throughout the 210–220 nm spectral region, indicative of a mixture of α-helix and β-structures. Quantitative analysis using CONTINLL indicated α-helical contents of 82 and 47 % at pH 5.0 in the presence of DMPG and DMPC respectively (Table 2). Whereas the β-structures account for 35 % in DMPC and 6 % in DMPG at pH 5.0, when the pH is raised to 7.4, the peptide adopts significantly fewer α-helical conformations with helicity of 65 % in DMPG and 16 % in DMPC. In contrast, the content of β-structure increased substantially to 20 % and 68 % in DMPG and DMPC respectively, whereas the amount of unordered structures remained almost unchanged (Table 2).

pH effects on the secondary structure of DMT1-TM4

The effects of pH on secondary structure were investigated in aq. 60 % TFE, with the results shown in Figure 5. The peptide exhibits the highest helical content (85 %) at pH 2.5. As the pH increases, the α-helical content decreases gradually, reaching a plateau at $\approx$ pH 6.0, and remains unchanged until pH 8.5 ($\approx$50 % α-helix). The titration curve gave rise to an associated pK_a value of 4.3.

Similarly, in the presence of 100 mM SDS at pH 2.5, the peptide has the highest α-helical content (77 %). As the pH increases, the α-helical content decreases gradually and reaches a plateau at $\approx$ pH 7.4, with a pK_a value of $\approx$5.6 (Figure 5). The changes in α-helical contents over the range of pH studied are smaller than those in the TFE/water mixtures, indicating that the peptide

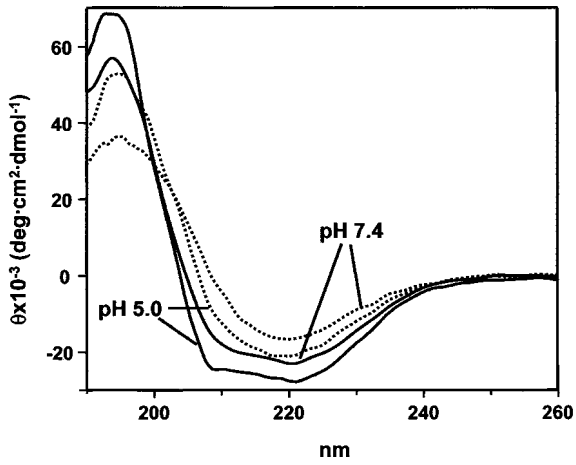

Figure 4 CD spectra of DMT1-TM4 in DMPC (dotted line) and DMPG vesicles (continuous line) at pH 5.0 and 7.4

The peptide concentration was 19 μM, and the lipid/peptide molar ratios were 200 : 1. The spectra were recorded at ambient temperature. Abbreviation: deg, degrees.

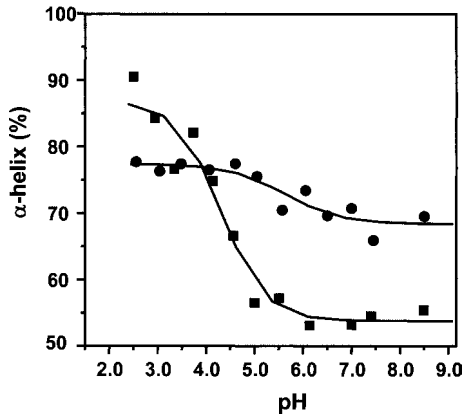

Figure 5 Effects of pH on secondary structure

The pH-dependence of the helicity of DMT1-TM4 (12 μM) in 60 % TFE/40 % water (■) and in 100 mM SDS (●).

adopts a more stable conformation in SDS micelles than that in TFE.

Temperature effects on the secondary structure of DMT1-TM4

The thermal stability of the DMT1-TM4 peptide in TFE and in 100 mM SDS was examined by raising the temperature in 5 °C increments, allowing equilibrium for 20 min prior to recording the CD spectra (Figure 6). The fraction of the peptide in an α-helical conformation was observed to decrease almost linearly with temperature, from 72 % at 5 °C, to 55 % at 60 °C in TFE. Upon cooling of the sample, the original spectra were recovered (results not shown), indicating that it was a fully reversible process. Unlike in the TFE system, in the presence of 100 mM SDS the helicity of the peptide decreased only slightly when the temperature was raised from 5 to 70 °C, namely 76 % compared with 70 % respectively, again suggesting that the peptide exhibits a more stable structure in SDS micelles.

NMR studies of secondary structure of DMT1-TM4 in SDS micelles

NMR sequence-specific resonance assignment for DMT1-TM4 was made by the combined use of TOCSY and NOESY spectra,

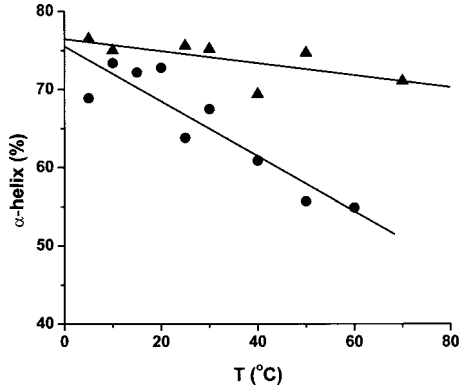

Figure 6 Effects of temperature on secondary structure

The helicity of DMT1-TM4 as a function of temperature in TFE (●) and SDS (▲).

following the sequential assignment strategy [37]. The most residues are well resolved in the TOCSY spectrum of DMT1-TM4 in the presence of 300 mM [$^2H_{25}$]SDS at pH 4.0 and 25 °C, apart from Thr[15] and Asp[22], which are partially overlapped with Leu[19] and Tyr[24] respectively. Residues Val[2], Asp[22], Lys[23] and Tyr[24] appear to give rise to the most intense signals, whereas residues from Gly[6] to Val[17] are less intense. In particular, the Asp[14] signal was very weak (results not shown).

The difference between the Hα proton chemical shifts (δ) in a protein and the chemical shifts in a random coil was known to correlate well with protein secondary structure. An α-helix structure is indicated by an upfield chemical shift of more than 0.1 p.p.m. with respect to random-coil chemical-shift values [38]. Figure 7(A) shows a graph of the Hα secondary chemical shifts ($\Delta\delta = \delta - \delta_{rc}$, where rc means random coil) of DMT1-TM4 in SDS micelles at pH 4.0. The results indicate that the peptide appears to adopt a helical structure from Val[8] extended to the C-terminal residue Tyr[24] with the N-termini highly disordered. This is also in close agreement with the observed NOE connectivities. The characteristic NOE connectivity pattern for an α-helix is the presence of medium range contacts such as H$\alpha(i)$–H$\beta(i+3)$, H$\alpha(i)$–HN$(i+3)$, H$\alpha(i)$–HN$(i+4)$ [39,40]. On the basis of resonance assignments, a large number of sequential and medium-range NOE cross-peaks can be identified in the NOESY spectra. Some of the medium-range NOE connectivities are summarized and shown in Figure 7(B). It can be seen clearly from Figure 7(B) that the peptide is composed of two main segments. The N-terminal segment from Arg[1] to Gly[7] forms an extended conformation, whereas the α-helical segment comprises residues from Val[8] to Lys[23], which will give rise to $\approx$67 % helicity, findings consistent with those obtained from our CD simulations.

Positioning of DMT1-TM4 in SDS micelles

To determine the orientation of DMT1-TM4 with respect to the micelle surface, the spin labels of 5- and 16-doxylstearic acids were used to produce selective broadening of the proton resonances from amino acid residues close to the spin label. These spin labels contain doxyl headgroups, a cyclic nitroxide with unpaired electrons, which is covalently linked to the aliphatic-chain carbon atom in position 5 or 16 respectively. The average position of the spin labels in the micelles has been derived previously from the line-broadening of the resonances in the ^{13}C spectrum of SDS. The doxyl group of 16-doxylstearic acids was found to be located mostly around the micelle centre, whereas the

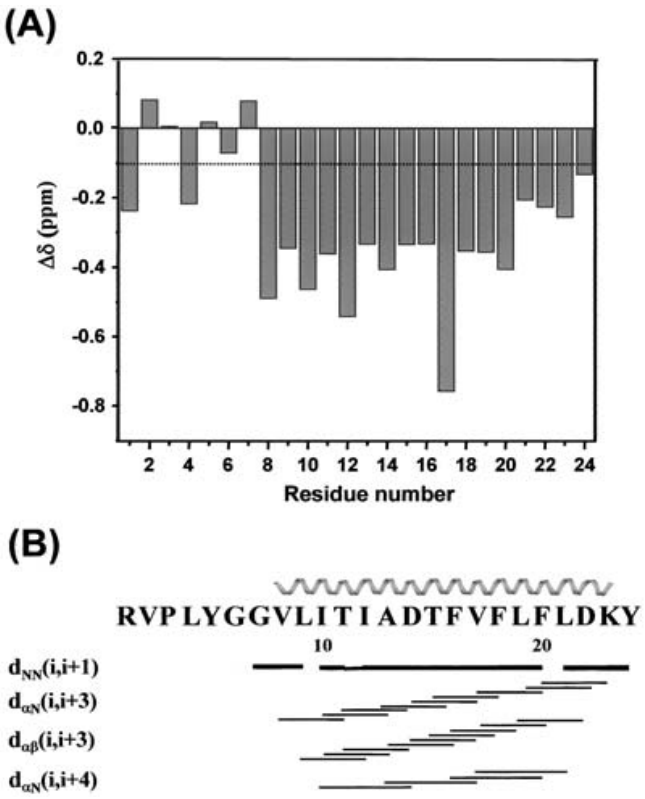

Figure 7 Secondary-structure studies by NMR spectroscopy

(**A**) Difference between the Hα chemical shifts observed and the random-coil chemical shifts in Wüthrich [37] is represented as a function of residue number in SDS micelles at pH 4.0. (**B**) Medium-range NOE contacts observed in the NOESY spectrum of DMT1-TM4 in SDS micelles at pH 4.0, 25 °C. $d_{NN}(i,i+1)$ is the distance between adjacent amide proteins.

5-doxylstearic acid is located close to the phosphate group at the micelle surface [41–44].

The spin labels were added to yield a molar ratio of spin labels to detergent of 1 : 60, which provides an average occurrence of approximately one molecule of the relaxation reagents per micelle. The effects of the spin labels on the peptide in the micelles were measured by comparing the cross-peak intensities in the TOCSY spectra in the absence and presence of the spin labels. The amplitudes of the spectra in the presence of the spin labels were normalized to the least affected cross-peaks, which allows evaluation of the effects from the spin labels semi-quantitatively. It was shown that the presence of 16-doxylstearic acid caused a complete disappearance of TOCSY cross-peaks of the residues located around the hydrophobic core of the peptide, e.g. residues of Ile[12], Ala[13], Asp[14] and Phe[16], while the cross-peaks for residues Gly[6], Gly[7], Val[8], Ile[10], Thr[11], Thr[15], Phe[18], Leu[19], Phe[20] and Leu[21] decreased their intensities moderately, and the intensities for the cross-peaks of Leu[9] and Val[17] fell significantly (Figure 8). Analogous changes were observed in the Hα–Hβ region of the spectrum (results not shown). This clearly indicated that the peptide has inserted into the interior of SDS micelles. The residues from Gly[6] to Phe[20] retained their intensities of $\approx$60 to 90 %, except residues Val[8], Ile[10] and Ala[13] in the presence of 5-doxylstearic acid (Figure 8). We considered that these residues were slightly affected by 5-doxylstearic acid, since the uncertainties may arise in the qualification of the intensities of two-dimensional cross-peaks, especially in the presence of spin labels. We can conclude from our combined spin-label experiments that the overall effects on residues Gly[6] to Phe[20]

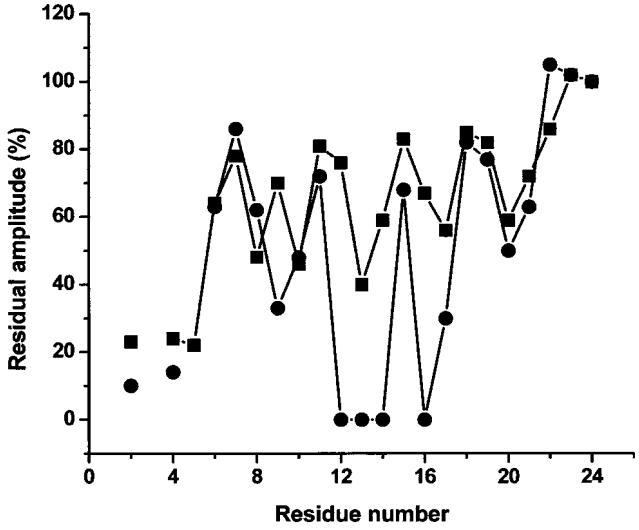

Figure 8 Insertions of DMT1-TM4 into SDS micelles

Residual relative intensities of HN–Hα TOCSY cross-peaks of DMT1-TM4 in SDS micelles after addition of 5 mM 16-doxylstearic acid (●) and 5-doxylstearic acid (■).

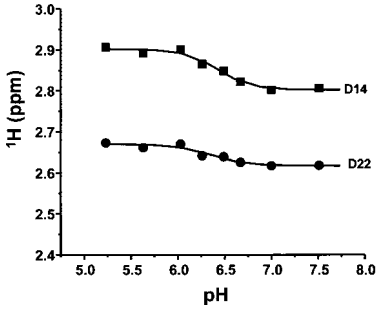

Figure 9 Changes in side-chain chemical shifts of Asp^{14} (D14) and Asp^{22} (D22) with pH

The average of the two β-proton chemical shifts is shown. The titration curves give rise to pK_a values of $\approx$6.4 for side chains of both aspartic acid residues.

from 5-doxylstearic acid were lesser in extent compared with that from 16-doxylstearic acid, which again suggested that the peptide was inserted in the interior of SDS micelles rather than lying on the surface of the micelles. The C-terminal residues such as Asp^{22}, Lys^{23} and Tyr^{24} were unaffected by the presence of both 5- and 16-doxylstearic acids (Figure 8), indicating that the C-terminus was exposed outside SDS micelles in the aqueous phase. Surprisingly, the cross-peaks for the N-terminal residues, e.g. Val^2, and Leu^4, decreased their intensities significantly upon addition of both 5- and 16-doxylstearic acid. Therefore it appears that the N-terminus might bend to insert in the micelles.

In order to verify further that the DMT1-TM4 peptide has indeed inserted into SDS micelles, the pK_a values for the side-chain groups of Asp^{14} and Asp^{22} in the presence of SDS were measured from the pH-dependence of two-dimensional cross-peaks of their side chains to be $\approx$6.4 (Figure 9), which are much higher than the pK_a for the side chain of Asp in aqueous solutions (p$K_a \approx 4.0$). Higher pK_a values are likely due to the side chains of Asp^{14} and Asp^{22} experiencing either hydrophobic or electron-enriched environments.

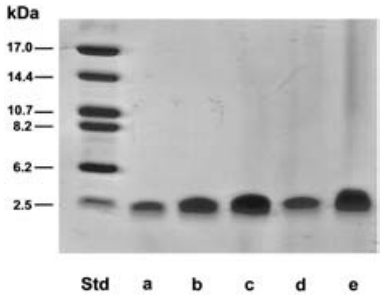

Figure 10 SDS/PAGE of DMT1-TM4

The peptide, dissolved in 0.5 % SDS, was diluted with 4×sample buffer and was boiled for 5 min prior to electrophoresis. A total of 20 μl of sample was loaded on to a 16.5 %-(w/v)-polyacryalamide gel using a Tricine buffer system. Peptide concentrations in each lane were as follows: lane a, 10 μM; lane b, 40 μM; lane c, 80 μM; lane d, 20 μM; lane e, 160 μM. Abbreviation: Std, molecular-mass standards.

Oligomeric state of DMT1-TM4 in SDS micelles assessed by Tricine/SDS/PAGE

SDS/PAGE was carried out to assess the molecular size of the DMT1-TM4 peptide in the presence of detergent micelles. This method has been widely used to examine the association of transmembrane domains, as SDS detergent micelles mimic the membrane environment [12,20,45,46]. The DMT1-TM4 peptide, incorporated into 17 mM (0.5 %) SDS/10 mM Tris buffer, pH 7.4, was electrophoresed on a 16.5 %-polyacryalamide gel utilizing a Tricine buffer system (Figure 10). In order to investigate whether the peptide concentration would affect its aggregation behaviour, we varied the peptide concentrations from 10 to 160 μM in different lanes of the gel (Figure 10). It can be seen clearly that the peptide migrated to an almost identical position near the bottom of the gel for each of concentrations studied, suggesting a monomeric form (molecular mass 2.7 kDa) in each case. Similar results were also obtained when the peptide was incorporated into 100 mM SDS, although a significant amount of band-broadening occurred (results not shown). Furthermore, no differences in migration patterns were observed whether or not the electrophoresis samples were subject to boiling prior to loading (results not shown), indicating that the peptide is thermally stable.

DISCUSSION

DMT1 plays a key role in iron homoeostasis, and it has been proposed that DMT1-TM4 is crucial for the function of DMT1 [10,11]. However, there has been no structural characterization of either the integral protein or this domain. In the present study we have investigated possibly structural aspects of DMT1-TM4 through studying a synthetic peptide in various membrane-mimetic environments. Synthetic membrane-mimicking peptides have been demonstrated to be extremely useful models to investigate not only structure, but also assembly and folding, of organized membrane regions of proteins [47–50]. It has been shown that the incorporation of M2 channel-lining segments in lipid bilayers reconstitutes functional cation-selective channels for both nicotinic acetylcholine and *N*-methyl-D-aspartate ('NMDA') subtype glutamate receptor [15]. Studies of peptide models of the membrane-spanning sequences of bacteriorhodopsin [19] and glycophorin A [16,51,52], membrane proteins of known three-dimensional structures, indicate that the folding of these proteins is largely dictated by interactions within the membrane and can occur in the absence of the remainder of

the protein. Our present studies are therefore likely to provide structural information related to the intact TM4 in integral DMT1.

CD spectroscopy is a well-established technique for studying the secondary structure of proteins and peptides. Its high sensitivity allows the conformational changes induced by changes of the environment to be monitored. Such changes are frequently observed when peptides largely unordered in aqueous solution partition into micelles or lipid bilayers [53,54]. The DMT1-TM4 peptide is composed of almost 70% hydrophobic amino acids and is insoluble in aqueous solutions and commonly used organic solvents. Therefore, we have chosen various solvents, including TFE, detergents (SDS and DPC) and phospholipids (DMPG and DMPC) to solubilize the peptide. In addition, these solvents may also serve as good models to mimic biological membranes [55]. Our results showed that the peptide adopts predominantly α-helical conformations in all amphiphilic environments studied, although there were trivial differences in the shapes of the spectra obtained. Analysis of the CD spectra gave rise to the highest helicity in DMPG vesicles (82%) and slightly lower helicity in SDS (73%), DPC (75%) and TFE (67%) and the lowest helicity in DMPC vesicles (47%) (Table 2). In contrast to previous reports [18], the effect of the charge of the detergent (SDS and DPC) micelles on the secondary structure of the peptide cannot be detected by CD spectroscopy. However, the negatively charged phospholipid DMPG promotes substantially more helical conformations for the DMT1-TM4 peptide than the zwitterionic DMPC. This finding is consistent with previous studies [54,56]. It was expected that hydrophobic interactions and electrostatic attractions between charged residues (often positively) and negatively charged lipids are often involved in most peptide–protein/lipid-binding processes [57,58]. Our results strongly suggest that primary electrostatic attractions provided by anionic phospholipids (DMPG) are essential for driving the DMT1-TM4 peptide to the membrane surface to achieve primary binding. Subsequent hydrophobic interactions with the lipid fatty acyl chains may then stabilize the peptide–membrane interaction and affect peptide insertions.

Although studies of secondary structure of membrane peptides by means of CD spectroscopy have many advantages, uncertainty may arise from the deconvolution of the CD spectra based on the method normally performed for globular proteins. Therefore, NMR spectroscopy was also used to investigate the secondary structures of DMT1-TM4 in SDS micelles. From both Hα secondary chemical shifts and NOE patterns, the α-helical segment comprising residues Val^{8}–Lys^{23} was estimated in SDS micelles at pH 4.0. The helicity obtained from both CD and NMR spectroscopies is in a very good agreement, which suggests that the method we used to extract the helical fraction is reliable.

The effects of pH on the secondary structure of DMT1-TM4 were also investigated in various media. This is of critical importance, as DMT1 transports divalent-metal ions only at the intracellular pH of about 5.5, but not at the extracellular pH of 7.4 [7,7a]. Furthermore, DMT1-mediated metal transport is a proton-coupled process, although it is not clear whether proton and divalent-metal ions are transported simultaneously or consecutively [7,7a]. Our results showed that the helicity decreased as pH was raised. The pK_a values of $\approx$4.3 and 5.6 were obtained in aq. TFE and in SDS micelles respectively (Figure 5). The difference may be attributable to the difference in the nature of the interaction between membrane peptides and amphiphilic solvents. Similarly, the secondary structure of DMT1-TM4 in phospholipids is also different at pH 5 and 7.4 (Table 2). Such a pH-induced conformational change has been observed previously [59–61], for example in the fusion domain of the influenza haemagglutinin. It was shown that this domain has a sharper bend at the fusogenic pH 5 than at the non-fusogenic pH 7.4, allowing a deeper insertion of the fusion domain into the core of the lipid bilayer [59]. It remains to be seen whether functional role of transmembrane domain 4 is also achieved through a pH-induced shift in its structure.

The orientation and topology of membrane protein is an important aspect of the overall structure that underlines the function of these proteins. A number of techniques are available to probe the locations of protein segments with respect to the lipid bilayers or detergent micelles, such as fluorescence, ESR and NMR. The topology study by means of fluorescence in this study was hampered due to the lack of tryptophan residues in the peptide. The membrane location of DMT1-TM4 in SDS micelles was therefore probed by the distance-dependent effect of spin labels (5- and 16-doxylstearic acids) on cross-peak intensities in TOCSY spectra. However, caution must be taken in analysis and interpretation of these data, since it is difficult to precisely quantify the cross-peaks of two-dimensional spectra, particularly in the presence of spin labels. We have attempted to analyse the spectra using different references; the deviation between the relative residual signal amplitudes derived from these references are relatively large. Therefore we could only evaluate the amplitudes in Figure 9 semi-quantitatively. Nevertheless, we ascertained from Figure 9 that the most part of DMT1-TM4 was likely inserted into the interior of SDS micelles, since the intensities of the hydrophobic core of DMT1-TM4 (Ile^{12}, Arg^{13}, Asp^{14} and Phe^{16}) were drastically reduced by the presence of 16-doxylstearic acid, while there was little effect on these residues upon addition of 5-doxylstearic acid. This is similar to those peptides which assumed transmembrane orientations [41,42], but is in contrast with those peptides lying to the surface of detergent micelles, for which the intensities of the peptides are significantly affected by the presence of 5-doxylstearic acid but not 16-doxylstearic acid [62,63]. Secondly, the C-terminus appeared to be present outside of micelles in the aqueous phase, because the intensities of cross-peaks for the C-terminal residues were almost unaffected upon addition of both spin labels. The elevated pK_a value (6.4) of the side chain of Asp^{14} is also in agreement with our spin-label experiments that Asp^{14} is likely located in the hydrophobic interior, whereas Asp^{22} might be located outside of the micelles, but near the electron-rich headgroup of SDS. Such an insertion appears to be energetically favourable, since most of the residues of DMT1-TM4 are hydrophobic, while the C-terminus is hydrophilic. Curiously, unlike those of the C-terminus, which were unaffected by either 5- or 16-doxylstearic acids, the resonances of the N-terminus (e.g. Val^{2} and Leu^{4}) appeared to be affected by both spin labels i.e. 5- and 16-doxylstearic acids. This kind of phenomenon has been noticed previously when using spin-label broadening to study membrane peptide orientations in micelles [43,44]. Although there is no clear explanation for these observations, a possible specific interaction between the peptide and spin labels might be one of the reasons. Furthermore, unusual dynamic and a static disorder for certain residues in the peptide may also have contributions. Therefore, caution has to be taken in the interpretation of spin-label effects in peptide–micelle complexes. Presently, we are unable to form a firm opinion about the exact position of the N-terminus of DMT1-TM4 in the micelles. It is likely that the N-terminus might be bent to insert into micelles owing to a possibly flexible structure in this part based on the NOE patterns (Figure 7B). However we cannot exclude the possibility that it might locate at the water/detergent interface as a consequence of the favourable interaction between positively charged N-terminus and the negatively charged SDS.

The aggregation behaviour of the peptide in SDS (17 and 100 mM) detergent micelles was examined by SDS/PAGE utilizing a Tricine buffer system. Our results showed that no self-association has been detected for DMT1-TM4 under the conditions studied, and it exists in the monomeric state with an observed molecular masses of about 2.7 kDa. However, we cannot rule out the possibility of a weak interaction between DMT1-TM4 monomers, which might be undetectable when running the SDS-containing gel. Previous studies on the characterization of transmembrane domains of cystic fibrosis conductance regulator (CFTR) and *Saccharomyces cerevisiae* G-protein-coupled receptor (Ste2p receptor) demonstrated that some transmembrane domains tend to aggregate as oligomers, whilst others prefer to exist as monomeric structures in SDS micelles [12,20]. A recent study [46] suggested that certain transmembrane domains are responsible for the oligomerization of integral membrane proteins, as required for their function. Therefore further investigations into the oligomeric states of other TM domains of DMT1 are warranted in order to gain a better understanding of the native oligomeric state of this integral membrane protein.

In conclusion, the results presented here represent the first analysis of the secondary structure and orientation of DMT1-TM4 in membrane-mimetic environments. The DMT1-TM4 peptide adopts predominantly α-helical conformations in TFE, detergent micelles (SDS and DPC), and phospholipid vesicles (DMPC and DMPG). The helicity of the peptide was found to be influenced by a number of factors such as pH, temperature, the concentration of detergents and the charge of the lipids. CD studies demonstrated that the secondary structure of DMT1-TM4 is similar in TFE, in SDS or DPC micelles, and in negatively charged DMPG phospholipid vesicles. The content of α-helix obtained from NMR data is in agreement with that from CD simulations. The peptide was estimated from NMR analysis to adopt a helical conformation from Val^{8} to Lys^{23} in SDS micelles at pH 4.0 with the N-terminal highly disordered. DMT1-TM4 is able to attain transmembrane orientation, i.e. penetrating into the hydrophobic interior upon interaction with detergent micelles. This might be important for the possible functional role of this domain. It would be of interest to study the three-dimensional structure of the DMT1-TM4 peptide in different environments at different pH values in the future.

This work is supported by a Hong Kong Research Grants Council (RGC) grant (BQ-445) and by Hong Kong Polytechnic University Research Grants (G-YW 47 and A-PC 23). We thank the University of Hong Kong [Committee on Research and Conference Grants (CRCG) and University Research Grants (URG)] and the Area of Excellence Scheme of the University Grants Committee (Hong Kong) for their support. We thank Professor Charles M. Deber (Division of Structural Biology and Biochemistry, Research Institute, Hospital for Sick Children, Toronto, Canada) and Professor Fred Naider (Department of Chemistry, College of Staten Island of the City University of New York, New York, NY, U.S.A.) for advice on synthesis and purification of hydrophobic membrane peptides.

REFERENCES

1 Richardson, D. R. and Ponka, P. (1997) The molecular mechanisms of the metabolism and transport of iron in normal and neoplastic cells. Biochim. Biophys. Acta **1331**, 1–40
2 Qian, Z. M., Wang, Q. and Tang, P. L. (1997) Iron crossed the endosomal membrane by a carrier-mediated process. Prog. Biophys. Mol. Biol. **67**, 1–15
3 Sun, H. Z., Li, H. Y. and Sadler, P. J. (1999) Transferrin as a metal ion mediator. Chem. Rev. **99**, 2817–2842
4 Li, H. Y., Sun, H. Z. and Qian, Z. M. (2002) The role of the transferrin–transferrin-receptor system in drug delivery and targeting. Trends Pharmacol. Sci. **23**, 206–209
5 Andrews, N. C. (1999) Disorders of iron metabolism. New Engl. J. Med. **341**, 1986–1995
6 Smith, M. A., Harris, P. L. R., Sayre, L. M. and Perry, G. (1997) Iron accumulation in Alzheimer disease is a source of redox-generated free radicals. Proc. Natl. Acad. Sci. U.S.A. **94**, 9866–9868
7 Gunshin, H., Mackenzie, B., Berger, U. V., Gunshin, Y., Romero, M. F., Boron, W. F., Nussberger, S., Gollan, J. L. and Hediger, M. A. (1997) Cloning and characterization of a mammalian proton-coupled metal-ion transporter. Nature (London) **388**, 482–488
7a Fleming, M. D., Trenor, C. C., Su, M. A., Foernzler, D., Beier, D. R., Dietrich, W. F. and Andrews, N. C. (1997) Microcytic anemia mice have a mutation in Nramp2, a candidate iron transporter gene. Nat. Genet. **16**, 383–386
8 Feder, J. N., Gnirke, A., Thomas, W., Tsuchihashi, Z., Ruddy, D. A., Basava, A., Dormishian, F., Domingo, Jr, R., Ellis, M. C., Fullan, A. et al. (1996) A novel *MHC* class I-like gene is mutated in patients with hereditary haemochromatosis. Nat. Genet. **13**, 399–408
9 Donovan, A., Brownlie, A., Zhou, Y., Shepard, J., Pratt, S. J., Moynihan, J., Paw, B. H., Drejer, A., Barut, B., Zapata, A. et al. (2000) Positional cloning of zebrafish *ferroportin 1* identifies a conserved vertebrate iron exporter. Nature (London) **403**, 776–781
10 Fleming, M. D., Romano, M. A., Su, M. A., Garrick, L. M., Garrick, M. D. and Andrews, N. C. (1998) Nramp2 is mutated in the anemia Belgrade (b) rat: evidence of a role for Nramp2 in endosomal iron transport. Proc. Natl. Acad. Sci. U.S.A. **95**, 1148–1153
11 Su, M. A., Trenor, C. C., Fleming, J. C., Fleming, M. D. and Andrews, N. C. (1998) The G185R mutation disrupts function of the iron transporter Nramp2. Blood **92**, 2157–2163
12 Xie, H., Ding, F. X., Schreiber, D., Eng, G., Liu, S. F., Arshava, B., Arevalo, E., Becker, J. M. and Naider, F. (2000) Synthesis and biophysical analysis of transmembrane domains of a *Saccharomyces cerevisiae* G protein-coupled receptor. Biochemistry **39**, 15462–15474
13 Ding, F. X., Xie, H., Arshava, B., Becker, J. F. and Naider, F. (2001) ATR-FTIR study of the structure and orientation of transmembrane domains of the *Saccharomyces cerevisiae* α-mating factor receptor in phospholipids. Biochemistry **40**, 8945–8954
14 Sorgen, P. L., Hu, Y., Guan, L., Kaback, H. R. and Girvin, M. E. (2002) An approach to membrane protein structure without crystals. Proc. Natl. Acad. Sci. U.S.A. **99**, 14037–14040
15 Opella, S. J., Marassi, F. M., Gesell, J. J., Valente, A. P., Kim, Y., Oblatt-Montal, M. and Montal, M. (1999) Structures of the M2 channel-lining segments from nicotinic acetycholine and NMDA receptors by NMR spectroscopy. Nat. Struct. Biol. **6**, 374–379
16 MacKenzie, K. R., Prestegard, J. H. and Engelman, D. M. (1997) A transmembrane helix dimer: structure and implications. Science **276**, 131–133
17 Schulz, A., Bruns, K., Henklein, P., Krause, G., Schubert, M., Gudermann, T., Wray, V., Schultz, G. and Schöneberg, T. (2000) Requirement of specific intrahelical interactions for stabilizing the inactive conformation of glycoprotein hormone receptor. J. Biol. Chem. **275**, 37860–37869
18 Rozek, A., Friedrich, C. L. and Hancock, R. E. W. (2000) Structure of the bovine anti-microbial peptide indolicdin bound to dodecylphosphocholine and sodium dodecyl sulfate micelles. Biochemistry **39**, 15765–15774
19 Hunt, J. F., Earnest, T. N., Bousche, O., Kalghatgi, K., Reilly, K., Horvath, C., Rothschild, K. J. and Engelman, D. M. (1997) A biophysical study of integral membrane protein folding. Biochemistry **36**, 15156–15176
20 Wigley, W. C., Vijayakumar, S., Jones, J. D., Slaughter, C. and Thomas, P. J. (1998) Transmembrane domain of cystic fibrosis transmembrane conductance regulator: design, characterization, and secondary structure of synthetic peptides m1–m6. Biochemistry **37**, 844–853
21 Oblatt-Montal, M., Reddy, G. L., Iwamoto, T., Tomich, J. M. and Montal, M. (1994) Identification of anion channel-forming motif in the primary structure of CFTR, the cystic-fibrosis chloride channel. Proc. Natl. Acad. Sci. U.S.A. **91**, 1495–1499
22 Killian, J. A., Trouard, T. P., Greathouse, D. V., Chupin, V. and Lindblom, G. (1994) A general method for the preparation of mixed micelles of hydrophobic peptides and sodium dodecyl sulphate. FEBS Lett. **348**, 161–165
23 MacDonald, R. I. and MacDonald, R. C. (1975) Assembly of phospholipid vesicles bearing sialoglycoprotein from erythrocyte membrane. J. Biol. Chem. **250**, 9206–9214
24 Liu, L. P., Li, S. C., Goto, N. K. and Deber, C. M. (1996) Threshold hydrophobicity dictates helical conformations of peptides in membrane environments. Biopolymer **39**, 465–470
25 Bax, A. and Davis, D. G. (1985) MLEV-17-based two-dimensional homo-nuclear magnetization transfer spectroscopy. J. Magn. Reson. **65**, 355–360
26 Jeener, J., Meier, B. H., Bachmann, P. and Ernst, R. R. (1979) Investigation of exchange processes by two-dimensional NMR spectroscopy. J. Chem. Phys. **71**, 4546–4553
27 Piotto, M., Saudek, V. and Sklenar, V. (1992) Gradient-tailored excitation for single-quantum NMR spectroscopy of a aqueous solutions. J. Biol. NMR **2**, 661–665
28 Sreerama, N. and Woody, R. W. (2000) Estimation of protein secondary structure from circular dichroism spectra: comparison of CONTIN, SELCON, and CDSSTR methods with an expanded reference set. Anal. Biochem. **287**, 252–260
29 Provencher, S. W. and Glockner, J. (1981) Estimation of globular protein secondary structure from circular dichroism. Biochemistry **20**, 33–37
30 Wu, C. S. C., Ikeda, K. and Yang, J. T. (1981) Ordered conformation of polypeptides and proteins in acidic dodecyl sulfate solution. Biochemistry **20**, 566–570

31 Chen, Y. H., Yang, J. T. and Chau, K. H. (1974) Determination of the helix and β form of proteins in aqueous solution by circular dichroism. Biochemistry **13**, 3350–3359

32 Schägger, H. and von Jagow, G. (1987) Tricine sodium dodecyl sulfate polyacrylamide gel electrophoresis for the separation of proteins in the range from 1 kDa to 100 kDa. Anal. Biochem. **166**, 368–379

33 Zhong, L. X. and Johnson, Jr, W. C. (1992) Environment effects amino acid preference for secondary structure. Proc. Natl. Acad. Sci. U.S.A. **89**, 4462–4465

34 Watson, R. M., Woody, R. W., Lewis, R. V., Bohle, D. S., Andreotti, A. H., Ray, B. and Miller, K. W. (2001) Conformational changes in pediocin AcH upon vesicle binding and approximation of the membrane-bound structure in detergent micelles. Biochemistry **40**, 14037–14046

35 Lauterwein, J., Bosch, C., Brown, L. R. and Wüthrich, K. (1979) Physicochemical studies of the protein-lipid interactions in melittin-containing micelles. Biochim. Biophys. Acta **556**, 244–246

36 Wallace, B. A. and Mao, D. (1984) Circular dichroism analyses of membrane proteins – an estimation of differential light scattering and absorption flattening effects in large membrane vesicles and membrane sheets. Anal. Biochem. **142**, 317–328

37 Wüthrich, K. (1986) NMR of Protons and Nucleic Acids, Wiley, New York

38 Wishart, D. S., Sykes, B. D. and Richards, F. M. (1992) The chemical shift index: a fast and simple method for the assignment of protein secondary structure through NMR spectroscopy. Biochemistry **31**, 1647–1651

39 Wüthrich, K., Billeter, M. and Braun, W. (1984) Poly-peptide secondary structure determination by nuclear magnetic resonance observation of short proton-proton distance. J. Mol. Biol. **180**, 715–740

40 Billeter, M., Braun, W. and Wüthrich, K. (1982) Sequential resonance assignments in protein ^{1}H nuclear magnetic resonance spectra. Computation of sterically allowed proton–proton distance and statistical analysis of proton–proton distance in single crystal protein conformations. J. Mol. Biol. **155**, 321–346

41 Papavoine, C. H. M., Konings, R. N. H., Hilbers, C. W. and van de Ven, F. J. M. (1994) Location of M13 coated protein in sodium dodecyl sulfate micelles as determined by NMR. Biochemistry **33**, 12990–12997

42 Chupin, V., Killian, J. A., Breg, J., de Jongh, H. H. J., Boelens, R., Kaptein, R. and de Kruijff, B. (1995) PhoE signal peptide inserts into micelles as a dynamic helix–break–helix structure, which is modulated by the environment. A two-dimensional ^{1}H NMR study. Biochemistry **34**, 11617–11624

43 Jarvet, J., Zdunek, J., Damberg, P. and Gräslund, A. (1997) Three-dimensional structure and position of porcine motilin in sodium dodecyl sulfate micelles determined by ^{1}H NMR. Biochemistry **36**, 8153–8163

44 Lindberg, M., Jarvet, J., Langel, Ü. and Gräslund, A. (2001) Secondary structure and position of the cell-penetrating peptide transportan in SDS micelles as determined by NMR. Biochemistry **40**, 3141–3149

45 Avrahami, D., Oren, Z. and Shai, Y. (2001) Effect of multiple aliphatic amino acids substitutions on the structure, function, and mode of action of diastereomeric membrane active peptides. Biochemistry **40**, 12591–12603

46 Melnyk, R. A., Partridge, A. W. and Deber, C. M. (2001) Retention of native-like oligomerization states in transmembrane segment peptides: application to the *Escherichia coli* aspartate receptor. Biochemistry **40**, 11106–11113

47 Albert, A. D. and Yeagle, P. L. (2000) Domain approach to three dimensional structure of rhodopsin using high resolution nuclear magnetic resonance. Methods Enzymol. **315**, 107–115

48 Aggeli, A., Bannister, M. L., Bell, M., Boden, N., Findlay, J. B. C., Hunter, M., Knowles, P. F. and Yang, J. C. (1998) Conformational and ion-channeling activity of a 27-residue peptide modeled on the single-transmembrane segment of the IsK (minK) protein. Biochemistry **37**, 8121–8131

49 Martin, N. P., Leavitt, L. M., Sommers, C. M. and Dumont, M. E. (1999) Assembly of G protein-coupled receptor from fragments: Identification of functional receptors with discontinuities in each of the loops connecting transmembrane segments. Biochemistry **38**, 682–695

50 Ridge, K. D., Lee, S. S. and Yao, L. L. (1995) *In vivo* assembly of rhodopsin from expressed polypeptide fragments. Proc. Natl. Aacd. Sci. U.S.A. **92**, 3204–3208

51 Engelman, D. M., Steitz, T. A. and Goldman, A. (1986) Identifying nonpolar transbilayer helices in amino acid sequences of membrane proteins. Annu. Rev. Biophys. Biophys. Chem. **15**, 321–353

52 Adair, B. D. and Engelman, D. M. (1994) Glycophorin A helical transmembrane domains dimerize in phospholipid bilayers – a resonance energy transfer study. Biochemistry **33**, 5539–5544

53 Ladokhin, A. S., Selsted, M. E. and White, S. H. (1999) CD spectra of indolicidin antimicrobial peptides suggest turns, not polyproline helix. Biochemistry **38**, 12313–12319

54 Aivazian, D. and Stern, L. J. (2000) Phosphorylation of T cell receptor is ζ regulated by a lipid dependent folding transition. Nat. Struct. Biol. **7**, 1023–1026

55 Garavito, R. M. and Ferguson-Miller, S. (2001) Detergents as tools in membrane biochemistry. J. Biol. Chem. **276**, 32403–32406

56 Liu, L. P. and Deber, C. M. (1997) Anionic phospholipids modulate peptide insertion into membranes. Biochemistry **36**, 5476–5482

57 Kim, J. Y., Blackshear, P. J., Johnson, J. D. and Mclaughlin, S. (1994) Phosphorylation reverses the membrane association of peptides that correspond to the basic domains of MARCKS and neuromodulin. Biophys. J. **67**, 227–237

58 Breukink, E., Demel, R. A., de Korte-Kool, G. and de Kruijff, B. (1992) SecA insertion into phospholipids is stimulated by negatively charged lipids and inhibited by ATP – a monolayer study. Biochemistry **31**, 1119–1124

59 Han, X., Bushweller, J. H., Cafiso, D. S. and Tamm, L. K. (2001) Membrane structure and fusion-triggering conformational change of the fusion domain from influenza hemagglutinin. Nat. Struct. Biol. **8**, 715–720

60 Han, X. and Tamm, L. K. (2000) A host–guest system to study structure–function relationships of membrane fusion peptides. Proc. Natl. Acad. Sci. U.S.A. **97**, 13097–13102

61 Han, X. and Tamm, L. K. (2000) pH-dependent self-association of influenza hemagglutinin fusion peptides in lipids bilayers. J. Mol. Biol. **304**, 953–965

62 Bader, R., Bettio, A., Beck-Sickinger, A. G. and Zerbe, O. (2001) Structure and dynamics of micelle-bound neuropeptide Y: comparison with unligated NPY and implications for receptor selection. J. Mol. Biol. **305**, 307–329

63 Öhman, A., Lycksell, P., Juréus, A., Langel, Ö., Bartfai, T. and Gräslund, A. (1998) NMR study of the conformation and localization of porcine galanin in SDS micelles. Comparison with an inactive analog and a galanine receptor antagonist. Biochemistry **37**, 9169–9178

Received 7 January 2003/18 February 2003; accepted 19 March 2003
Published as BJ Immediate Publication 19 March 2003, DOI 10.1042/BJ20030075